

RESEARCH PAPER

ANALYZING TENSILE STRENGTH, HARDNESS, AND MICROSTRUCTURE OF INCONEL 625 AFTER QUENCHING THROUGH WATER, 3.5% NaCl, and 3.5% HCl

Ayush Agarwal, Abhisekh Modi, Nitesh Sharma, Saurabh Dewangan*

Department of Mechanical Engineering, Manipal University Jaipur, Jaipur, Rajasthan, India, Pin-303007

*Corresponding author: saurabh.dewangan@jaipur.manipal.edu, tel.: 0141-3999100-838, Department of Mechanical Engineering, Manipal University Jaipur, Jaipur, Rajasthan, India, Pin-303007

Received: 07.11.2024

Accepted: 23.11.2024

ABSTRACT

Inconel 625 is a high temperature bearing and corrosion resistant alloy. Its high strength, good hardness and remarkable ductility make this alloy widely used in aerospace, turbines, automotive, engine valves, fuel injectors, fasteners, etc. It is considered as heat treatable alloy. The present work deals with heating the Inconel 625 alloy to elevated temperature and cooling through quenching media, including water and chloride solutions. The tensile and hardness properties of the quenched samples were analyzed in the light of the 'untreated' sample available in 'cold-rolled' condition. The microstructural analysis was done using optical microscopy and FESEM. Apart from γ matrix and twin boundaries, Ti/Nb rich carbonitrides and needle- δ phases were reported in the treated samples. A slight corrosive degradation was also observed in the chloride-solution quenched samples. The XRD analysis proves the occurrence of oxide formation in Cr present at the γ grain boundary. As a result of quenching, the tensile and yield strength were reduced with a gain of overall elongation. Hence, quenching methods are beneficial for improving the ductile nature of Inconel 625 alloy, and hence, the hardness of the quenched products was found to be less than the 'as received' sample.

Keywords: Inconel 625; Heating; Quenching; Tensile properties; Hardness

INTRODUCTION

Because of its superior mechanical properties, Inconel-625 is a superalloy based on nickel-chromium widely used in the automotive, aerospace, petrochemical, and marine industries. It also provides excellent oxidation/corrosion protection [1]. Mo and Nb are utilised to increase hot strength, whilst chromium and molybdenum improve corrosion and oxidation resistance. Welding and brazing are used to bind the alloy together [2]. Inconel alloys are either precipitation hardened, or solid solution strengthened. 625 alloy comes under second category in which strengthening is done by the alloying elements like Mo/Cr/Nb and the elements such as C, N, and B act as reinforcing the interstitial sites [3-5]. In addition to solid solution strengthening, carbides are formed by metals such as Ti, Nb, Cr, and Mo and randomly disperse in phase. This alloy contains both γ' and γ'' . When Al content exceeds 0.5%, γ' prevails over γ'' [6, 7]. Increased particle size (γ') increases strength [8-10]. The alloy is primarily reinforced by organised γ'' precipitates and has a high nickel concentration. The alloy's predominantly γ'' composition results in fewer possible slip systems than γ' , which has more. The strength can be increased with decreasing the number of slip systems [11-18]. The formation of γ'' occurs at low temperatures (600-750 °C). It has been observed that orthorhombic phases develop at temperatures over 750 °C and dissolve above 1000 °C. Carbides can be found in samples aged for an extended time at temperatures ranging from 750 to 980 degrees Celsius. Carbides and intermetallic phases precipitate at ageing temperatures ranging from 550 to 980 °C [19]. Many research works are available on Inconel alloy which discuss deformation behaviour after hot compression, microstructural development in post-welded and post heat treated state, and various impacts of alloying components on the mechanical attributes [11-15, 20]. Various kinds of works have been carried on different grades of Inconel alloy. In a work, Inconel 718 plates were fabricated by laser metal deposition (LMD) method with addition of TiC contents. A fine distribution of TiC particles ensured high affinity between Nb and C and thereby the corrosion resistance was found higher in the fabricated alloy [21]. A discussion has been made to use the Inconel alloy into gas reactors because it can maintain its qualities up to 900 °C satisfactorily [22]. Inconel 690 was found to be more stable with chemical environment and hence its applicability gets enhanced in chemical industries [23]. A comparison among three metals, Haynes C276, 'AISI 316L', and 'Inconel 600' series alloy, was done by using them in the environment of LiCl-KCl salt as an electrolyte and liquid cadmium as a reactive material. Chemical oxidation was found to be the primary mechanism responsible for the predominance of steel degradation, accompanied by the notable phenomenon of severe nickel dealloying. The impact

of cadmium (Cd) on the penetrating behaviour of AISI 316L has been investigated. It has been observed that the presence of cadmium leads to the destabilization of the chromium (Cr) oxide layer. This leads to the creation of CdCrO₄ [24]. A study compares corrosion resistance in Hastelloy C-276, Inconel 600, and Monel 400, finding variations. Hastelloy C-276 is highly resistant, Inconel 600 has passivation film stability, but inclusions can degrade resistance. Copper's electrode potential and defect-free state are superior [25]. The phenomena of sensitization and stress corrosion were investigated by a sequence of heat treatments done on Inconel-690 alloy. The Huey test was conducted in a solution containing 65% boiling HNO₃. A period of 48 hours will be allocated to study the resistance of the alloy under investigation to intergranular assault (IGA). This examination demonstrated that Inconel 690 exhibits exceptional corrosion resistance properties [26]. Research work presents a comprehensive analysis aimed at enhancing the efficiency of the heat treatment procedure for Inconel 625 alloy. In the context of production, efforts are made to enhance the overall characteristics of the material. Implementing specialized treatment methods has been found to significantly enhance the corrosion resistance properties. The addition of alloy elements can enhance the material's flexibility while maintaining its strength [27]. As a result of hot corrosion effects on Inconel 718 alloy into the medium of salt mixture containing 87.5% Na₂SO₄, 5% NaCl, and 7.5% NaNO₃, the evidence of chromium oxidation was reported with formation of Cr₂O₃ as major depletion ingredient. Also, Fe₃O₄ and Ni₃S₂ were two additional compounds formed due to corrosion [28]. The NaCl solution treatment of welded joint of cast nickel alloy had shown both, the Laves phase and the carbides like NbC. Because of this, the welded joint was reported harder than base metal [29]. A study investigates the characteristics of hot extruded Inconel in the presence of Na₂SO₄ and V₂O₅, focusing on the alloying elements distribution. The analysis of molten salt systems was conducted through the utilization of XRD and SEM. This study provides evidence of rusting. The rate of increase in the alloy's temperature over time remains constant at a given temperature. The initial stage of corrosion was revealed by the presence of Cr₂O₃ and NiO. Upon a 24-hour immersion in the salt bath, a chemical interaction ensues between the alloy and its surroundings. The reaction between chromium (Cr) and vanadium (V) leads to the production of chromium vanadate (CrVO₄) and nickel vanadate (Ni₃V₂O₈). In addition, the incursion of the introduction of the sulphur (S) element into the matrix results in the creation of internal sulphides, such as those containing nickel (Ni), chromium (Cr), and so on [30]. Pitting corrosion phenomena were recorded during polarization tests at 3.56 % NaCl. Inconel's corrosion resistance was shown to be drastically reduced when exposed to 450 °C [31]. The use of A-USC-760°C alloy, which can be employed

at 760°C, is recommended for the power plants. Selecting a high temperature and pressure value is recommended for high efficiency [32, 33]. An increment of 10°C temperature can lead to 0.5% more efficiency in power plants because of burning less coal. As service pressure and temperature grew, power plants required materials with excellent creep strength. Inconel alloys are widely employed in such applications worldwide [34–37].

According to earlier literature, the Inconel alloy demonstrated good corrosion resistance when exposed to different chemicals, as stated above. Nevertheless, no prior research has documented the Inconel alloy's ability to withstand corrosion at a red-hot temperature. In this regard, the current study provides insight into the tensile behaviour, hardness, microstructure and corrosion attributes of Inconel 625 alloy after heat treatment and subsequent exposure to pure and acidic water environments.

MATERIAL AND METHODS

The experimental work involves heating the three Inconel-625 sheets of dimension 110×50×2.5 into a closed furnace. One more metal piece was taken in 'as received' condition. The heating temperature was fixed at 900°C for 15 min. Inconel 625 alloy, known for its strong temperature and chemical resistance, is widely used in various industrial applications, including reactor cores, jet engines, gas turbines, exhaust stacks, and steam heaters in the paper industry. The

temperature of the alloy can reach up to 750-1000°C during processing stages. Therefore, the current study utilizes 900°C for the Inconel samples under study. Three different quenching media were selected to cool these plates. The first was quenched in water, the second plate was dipped into 3.5% NaCl solution, and the third was quenched with 3.5% HCl solution. The quenching solutions were kept at room temperature (i.e. 28°C). Hence, the 'untreated' sample is named 'a', the water quenched sample is named 'b', the NaCl quenched sample is named 'c', and the HCl quenched plate is named 'd'. Because of quenching methods, various property changes may occur in the Inconel 625 alloy. The tensile properties were analyzed by performing a tensile test on a 'FIE make's tensile testing machine with 40 kN capacity. The standard specimens were prepared as mentioned by ASTM E8 guidelines. The tensile test specimens are shown in Fig. 1(a). Rockwell hardness test (C-scale) was carried out on the remaining plate. Five indents were made on each plate, and an average hardness value was determined. The microstructural attributes were observed through optical microscopy at the common magnification. A thorough preparation was followed to polish the samples with various grades of abrasive papers. Post-polishing work involved the etchant preparation. Nital etchant (2% nitric acid and ethanol) was applied to the polished surface before microstructure observation. The XRD analysis was done on each sample to verify the occurrence of corrosion due to chloride solution quenching. The observation and result analysis of each test have been discussed in the following sections:

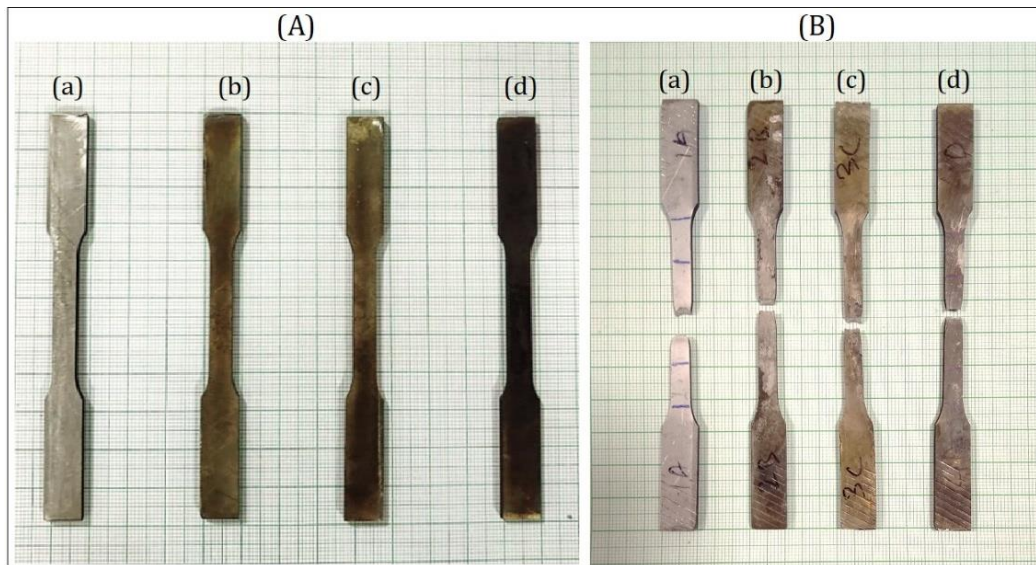


Fig. 1 (a) Specimens for tensile test; (b) fractured tensile specimens

RESULTS AND DISCUSSION

Tensile test: Fig. 1(b) shows the fractured tensile specimens. After the tensile test of each specimen, the load vs displacement values were recorded, and the graphs were plotted (Fig. 2). All the specimens got fractured nearly through the mid-section of the gauge. On the macroscopic observation, all the quenched specimens have shown higher stretching of the gauge section as compared with untreated sample. Sample *a* showed tensile strength (TS) of 957.65 MPa with a maximum elongation (E_f) of 19.4 mm. The yielding starts after 3 mm stretching. Therefore, the elongation until yielding (E_y) begins is 3 mm. The untreated sample has exhibited yield stress (YS) of 647.58 MPa. After quenching through three different media, the specimens lost the TS and YS. Sample *b* has reduced the TS by 4%. A significant 21% and 27% reduction has been noticed in the YS

and E_y upon water quenching. The E_f of the water quenched sample has increased by 17% in comparison to sample *a*. Sample *c*, being cooled by 3.5% NaCl solution, has lost the TS, YS, and E_y by 5%, 28%, and 43% respectively as compared to sample *a*. The overall elongation of sample *c* has increased by 16%. In sample *d*, the decrement of 4%, 27%, and 37% was recorded in TS, YS, and E_y respectively although the elongation till fracture has increased by 19%.

Hence, it can be observed that various quenching media have reduced the elastic limit of the samples. Both the tensile strength and yield strength have reduced due to quenching. The maximum elongation before fracture has increased as a result of quenching. The ductility of Inconel 625 increases with the quenching process. All the tensile properties are provided in Table 1. A comparative bar chart among various tensile properties is shown in Fig. 3.

Table 1 Tensile properties of four samples under study

S No	Sample	TS (MPa)	% change wrt sample (a)	YS (MPa)	% change wrt sample (a)	E_f (mm)	% change wrt sample (a)	E_y (mm)	% change wrt sample (a)
1	<i>a</i>	957.65	-	647.58	-	19.4	-	3	-
2	<i>b</i>	919.29	-4%	514.68	-21%	22.7	17%	2.2	-27%
3	<i>c</i>	907.88	-5%	466.99	-28%	22.5	16%	1.7	-43%
4	<i>d</i>	914.61	-4%	471.61	-27%	23.1	19%	1.9	-37%

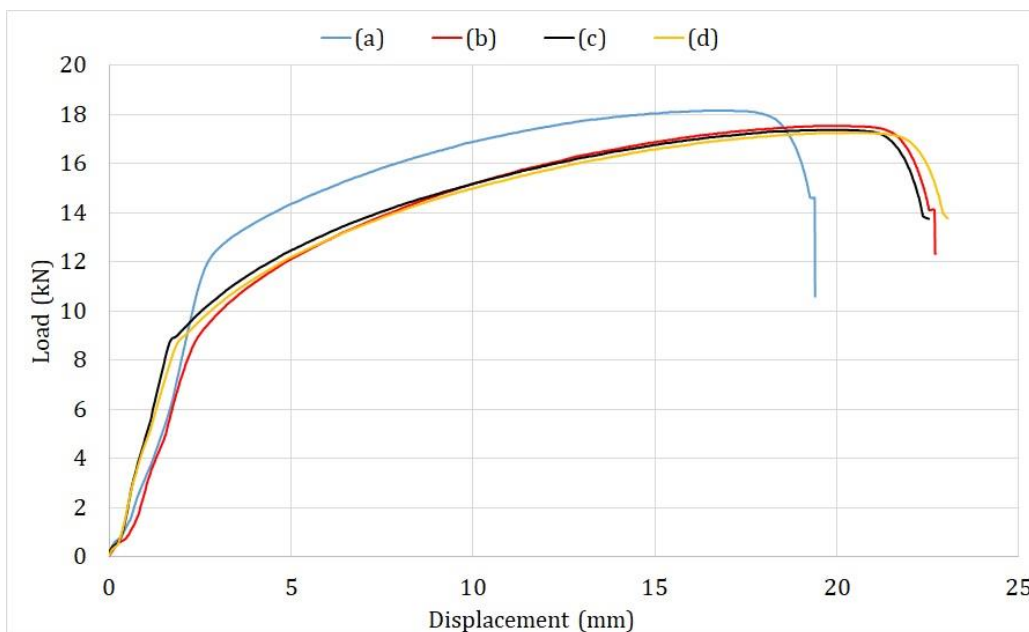


Fig. 2 Load- displacement graphs after the tensile test

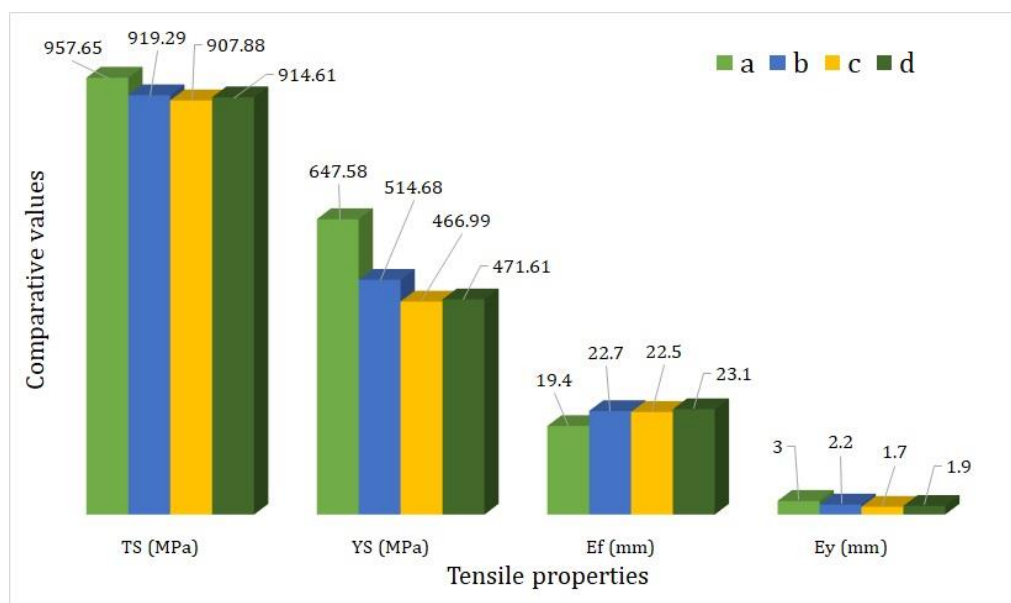


Fig. 3 Comparative assessment of tensile properties

Hardness test: The hardness at various points of four samples is written in Table 2. The average hardness of each plate is shown in Table 2. The hardness recorded in samples a, b, c, and d are 26.2 HRC, 22.6 HRC, 21.8 HRC and 21.6 HRC, respectively. The highest hardness was observed in the original sample,

whereas the three-quenching process reduced the hardness. This result established the tensile properties of quenched specimens in which the quenched specimens were found to be highly ductile. Fig. 4 shows a bar chart that compares the hardness of all samples.

Table 2 Hardness distribution at various points of samples

Sample	HRC-1	HRC-2	HRC-3	HRC-4	HRC-5	Average Hardness (HRC)
Original	25	25	26	31	24	26.2
Water quenched	19	23	24	24	23	22.6
3.5% NaCl quenched	20	19	21	26	23	21.8
3.5% HCl quenched	24	22	23	22	17	21.6

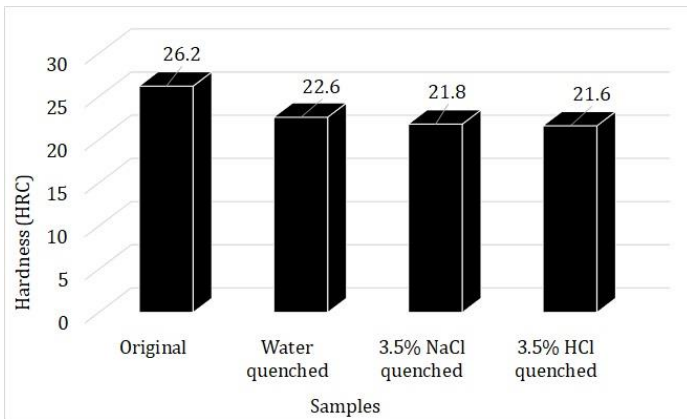


Fig. 4 A comparative bar chart of hardness at different samples

3.3 Microstructural analysis: The microstructure photographs of four samples are shown in Fig. 5. The images are taken on a scale of 50 μm . All the images have exhibited a similar appearance, like the bright appearance of γ -matrix, and fine back particles of metal carbides (possibly in the form of TiC, Cr_{23}C_6 , NbC, etc.) [38, 39]. Some twins were also reported in each sample, which generally form with the initiation of recrystallization so that interfacial energy can be

reduced [40]. Along with the small black dispersion of carbides, the gray coloured equiaxed shaped grains with black boundaries represent Nb/Ti rich carbonitride. These large carbides can reduce the fatigue strength and hence be responsible for crack initiation through γ grain boundaries. The formation of large carbonitrides can be avoided by choosing heat treatment methods [41]. In this work, the large carbonitride is absent in water quenched sample. However, the size of carbonitrides is coarser in sample *c* and *d* as compared to sample *a*. Hence, water quenching provides a favorable condition to reduce the possibilities of Nb/Ti rich carbonitride. According to [42] and [43], the quenching process can cause the movement of alloying elements towards the austenite grain boundary resulting in less strength of the individual austenite grain.

The high-magnification images of the microstructure have been captured by FESEM. FESEM images could easily identify the γ grains and their boundaries, Fig. 6. Twin formation was reported in all the samples. A new phase, i.e., δ -phase, considered Nb rich, was seen in every sample by its needle-like appearance near the grain boundaries and on individual γ grain. The δ -phase is referred as Nb-rich phase. It is an "ordered orthorhombic structure", manifests as long needles. Grain growth during solution and aging can be controlled using a little quantity of delta phase. On the other hand, excessive delta phase is harmful and can reduce strength, creep resistance, and fracture toughness [41]. Nb is alloyed with Inconel to slow down the growth of grains during solution treatment and aging [39, 41]. A coarse-shaped carbonitride was mainly reported in 3.5% NaCl quenched sample. In Fig. 6 (c) and Fig. 6 (d), a slight change in the grain boundary of γ was reported. These changes are caused by Cr depletion due to NaCl and HCl quenching.

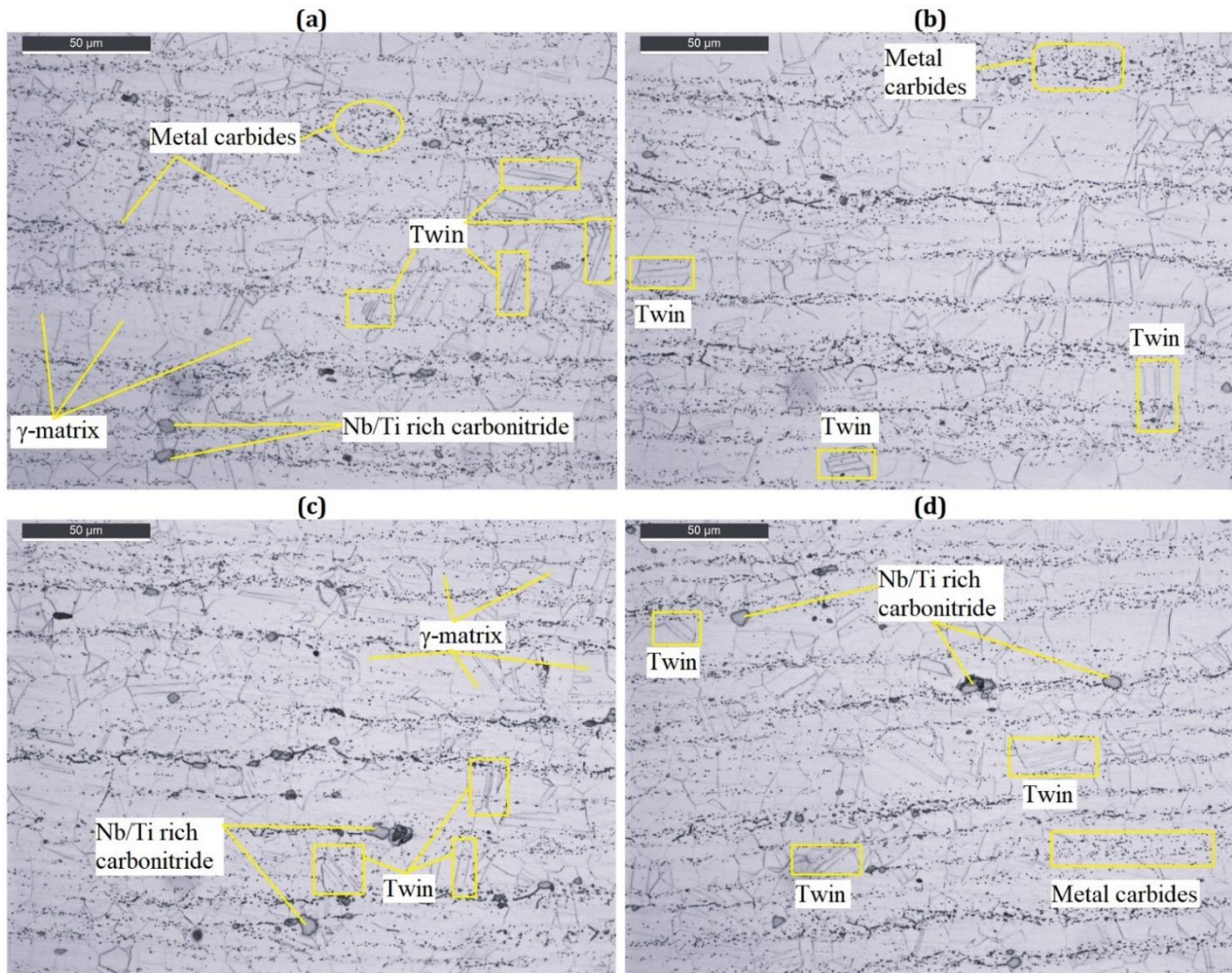


Fig. 5 Microstructure of 625 alloy by optical microscopy: (a) 'as received' sample; (b) 'water quenched' sample; (c) '3.5% NaCl quenched' sample; (d) '3.5% HCl quenched' sample

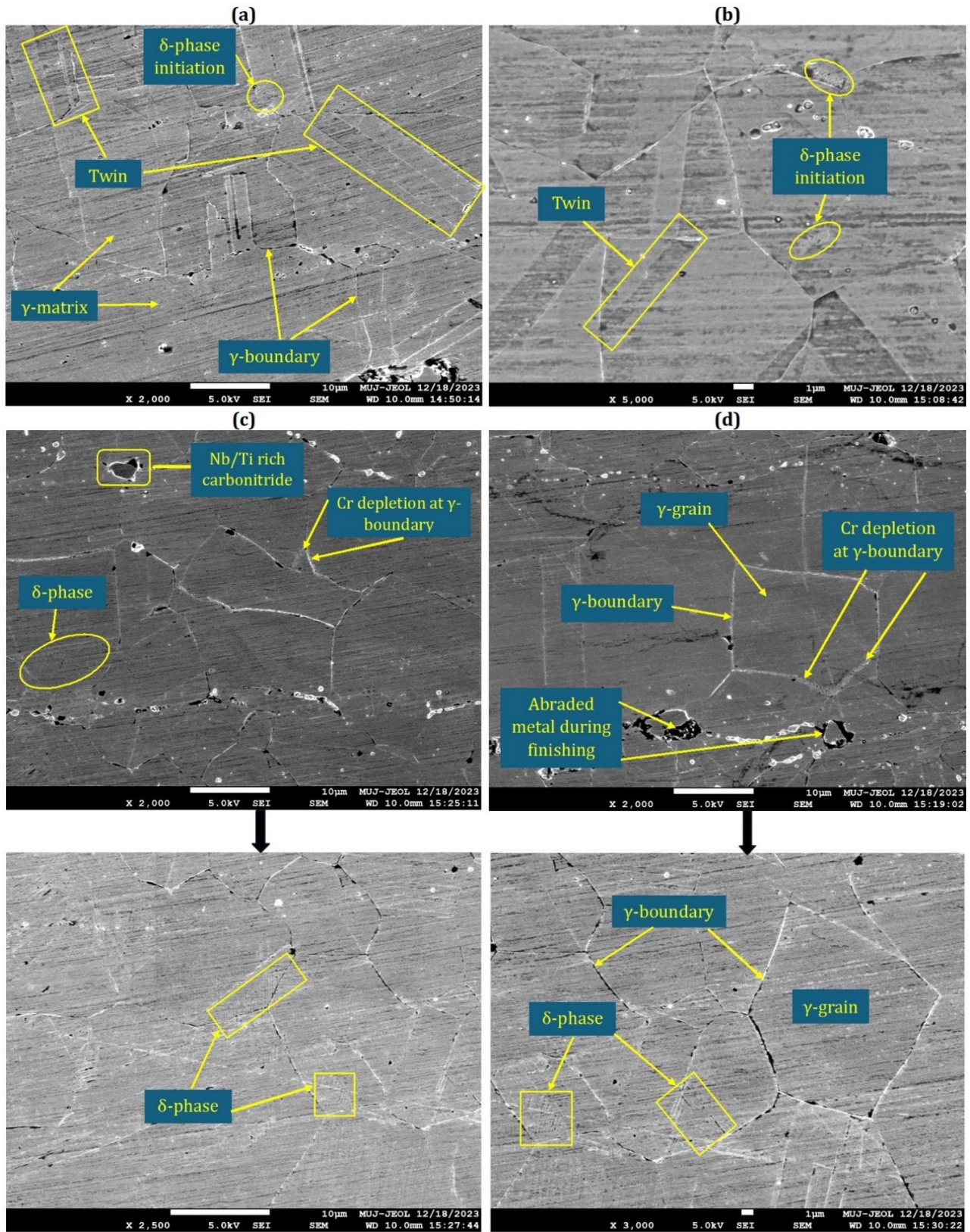


Fig. 6 Microstructure of 625 alloy by FESEM: (a) 'as received' sample; (b) 'water quenched' sample; (c) '3.5% NaCl quenched' sample; (d) '3.5% HCl quenched' sample

XRD analysis: To establish the corrosive degradation of 625 alloys in the chloride solution quenched samples, XRD analysis was carried out (Fig. 7). Based on previously reported work by [44] and [45], the range of 2θ varied between 30° to 80° . All the samples have shown three intense peaks of γ -matrix on the planes of (111), (200), and (220) at 2θ of 43° , 51° and 74° respectively. In addition, small peaks of Cr_2O_3 , as referred to by [45], have been obtained at two different 2θ of 37.5° and 63° in samples *c* and *d*. It establishes that the observation of Cr depletion at the γ boundary is due to NaCl and HCl's chemical attack in samples *c* and *d*, respectively.

According to [46], Cr depletion in Inconel alloy systems occurs when a chemical compound forms at the surface, removing chromium from the matrix. Oxide formation, liquid metal corrosion, sulfidation, heat treatment, and internal oxidation are some techniques through which Cr depletion occurs, leaving the base metal corroded.

Heat treatment may significantly reduce the dislocation density in the microstructure by removing dislocations and restoring cold-deformed material. By dissolving dendritic features, water quenching can lower the dislocation density and provide a uniform microstructure [47-49]. Further investigation is needed to check the dislocation density using a high-end instrument like transmission electron microscopy (TEM).

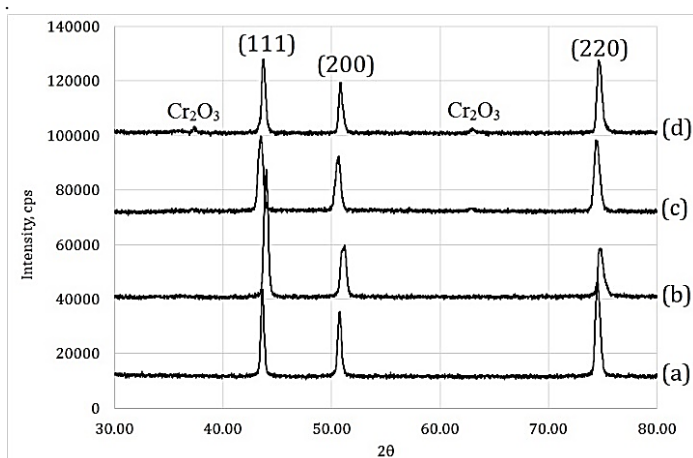


Fig. 7 XRD analysis of four Inconel plates under study: (a) 'as received' sample; (b) 'water quenched' sample; (c) '3.5% NaCl quenched' sample; (d) '3.5% HCl quenched' sample

CONCLUSION

Based on the tensile test, it was found that Inconel 625 alloy is a strong and ductile metal. It possesses tensile strength at a range of 957 MPa with nearly 19 mm of extension in gauge length before fracture. The quenching phenomenon has affected its tensile properties, such as TS, YS and elongation, till yielding. The three quenching methods have slightly reduced the TS by 4%, but the YS of the samples was reduced by more than 20%. The quenched samples' elastic limit is significantly reduced by more than 27%. Quenching methods have increased the elongation (till fracture). By analyzing these tensile properties, it can be concluded that quenching through water and chemical solution can increase the ductility of the Inconel 625 alloy with a loss of ultimate tensile strength.

The hardness results justify the tensile test results. After quenching, due to an increment in ductility, the average hardness of Inconel 625 alloy is lower than that of the 'untreated' sample.

The optical microscopy has shown structures like γ -matrix, fine back particles of metal carbides, twin formation, and Nb/Ti rich carbonitride. However, there was no difference reported at the microstructure level between untreated and treated Inconel alloy. At the high magnification of 2000X in FESEM, the presence of needle-shaped δ -phase could also be reported. The γ -grain boundary corrosion was seen through FESEM, further established by the chromium oxide (Cr_2O_3) peaks provided through XRD analysis. The oxide peaks of HCl quenched sample are predominant over the NaCl quenched sample.

Although NaCl and HCl solution quenching was done on the samples heated at 900°C , but less corrosive degradation was reported. Also, water does not affect the corrosion resistance of Inconel alloy, even at elevated temperatures.

REFERENCES

- [1] H.L. Eiselstein, D.J. Tillack: *Superalloys*, 718(625), 1991, 1-14. https://www.tms.org/superalloys/10.7449/1991/Superalloys_1991_1_14.pdf
- [2] S. Dewangan, S. Narayanan, G.S. Gill, U. Chadha: *Acta Metallurgica Slovaca*, 29(1), 2023, 5-9. <https://doi.org/10.36547/ams.29.1.1664>.
- [3] S. Dewangan, S.S.S. Sunder, Y. Bhadoriya, S. Mohite, A.P. Reddy: *Journal of The Institution of Engineers (India): Series D*, 2023, 1-12. <https://doi.org/10.1007/s40033-023-00578-4>.
- [4] M.E. Kassner, K.T. Son, K.A. Lee, T.H. Kang, R. Ermagan: *Materials at High Temperatures*, 39(6), 2022, 499-506. <https://doi.org/10.1080/09603409.2022.2045101>.
- [5] K.J. Irvine, F.B. Pickering: *Journal of the Iron and Steel Institute*, 201(6), 1963, 518. <https://doi.org/10.1007/BF03378721>.
- [6] V.G. Krishna, G.D. Janakiram, C.H.V.S. Murty, M. Srinivas, A.V. Reddy: *Practical Metallography*, 45(10), 2008, 495-504. <https://doi.org/10.3139/147.100399>.
- [7] S.S.S. Sunder, S. Dewangan: *Journal of The Institution of Engineers (India): Series D*, 2023, 1-9. <https://doi.org/10.1007/s40033-023-00537-z>.
- [8] D. Raynor, J.M. Silcock: *Metal Science Journal*, 4(1), 1970, 121-130. <https://doi.org/10.1179/msc.1970.4.1.121>.
- [9] J. D. Whittenberger: *Materials and Manufacturing Processes*, 7(3), 1992, 463-468. <https://doi.org/10.1080/10426919208947432>.
- [10] M. Zouari, N. Bozzolo, R.E. Loge: *Materials Science and Engineering: A*, 655, 2016, 408-424. <https://doi.org/10.1016/j.msea.2015.12.102>.
- [11] X. Xing, X. Di, B. Wang: *Journal of Alloys and Compounds*, 593, 2014, 110-116. <https://doi.org/10.1016/j.jallcom.2013.12.224>.
- [12] K.H. Song, K. Nakata: *Materials & Design*, 31(6), 2010, 2942-2947. <https://doi.org/10.1016/j.matdes.2009.12.020>.
- [13] J.B. Singh, A. Verma, D.M. Jaiswal, N. Kumar, R.D. Patel, J.K. Chakravarty: *Materials Science and Engineering: A*, 644, 2015, 254-267. <https://doi.org/10.1016/j.msea.2015.06.098>.
- [14] Q. Guo, D. Li, S. Guo, H. Peng, J. Hu: *Journal of Nuclear Materials*, 414(3), 2011, 440-450. <http://dx.doi.org/10.1016/j.jnucmat.2011.05.029>.
- [15] D. Li, Q. Guo, S. Guo, H. Peng, Z. Wu: *Materials & Design*, 32(2), 2011, 696-705. <http://dx.doi.org/10.1016/j.matdes.2010.07.040>.
- [16] J. Mitra, S. Banerjee, R. Tewari, G.K. Dey: *Materials Science and Engineering: A*, 574, 2013, 86-93. <http://dx.doi.org/10.1016/j.msea.2013.03.021>.
- [17] F. Xu, Y. Lv, Y. Liu, F. Shu, P. He, B. Xu: *Journal of Materials Science & Technology*, 29(5), 2013, 480-488. <http://dx.doi.org/10.1016/j.jmst.2013.02.010>.
- [18] A. Nagesha, P. Parameswaran, N. Kumar, R. Sandhya, M.D. Mathew: *Materials at High Temperatures*, 29(1), 2012, 49-53. <https://doi.org/10.3184/096034012X13269868036418>.
- [19] M.D. Mathew, P. Parameswaran, K.B.S. Rao: *Materials Characterization*, 59(5), 2008, 508-513. <https://doi.org/10.1016/j.matchar.2007.03.007>.
- [20] A. Sukumaran, R.K. Gupta, V. Anil Kumar: *Journal of Materials Engineering and Performance*, 26, 2017, 3048-3057. <https://doi.org/10.1007/s11665-017-2774-8>.
- [21] D. Kong, S. Dong, X. Ni, L. Zhang, C. Man, G. Zhu, J. Yao, L. Wang, X. Cheng, X. Li: *Journal of Alloys and Compounds*, 803, 2019, 637-648. <https://doi.org/10.1016/j.jallcom.2019.06.317>.
- [22] D. Marušáková, C.A. Corrêa, C. Aparicio, O. Libera, J. Berka, M. Vilémová, P. Gávelová: *Coatings*, 13(1), 2022, 45. <https://doi.org/10.3390/coatings13010045>.
- [23] C. Liu, W. Yao, S. Shang, K. Guo, H. Sun, C. Liu: *Coatings*, 13(2), 2023, 340. <https://doi.org/10.3390/coatings13020340>.
- [24] Y. Jia, S. Chang, X. Du, S. Guo: *Crystals*, 13(5), 2023, 817. <https://doi.org/10.3390/cryst13050817>.
- [25] H. Dai, S. Shi, L. Yang, J. Hu, C. Liu, C. Guo, X. Chen: *Corrosion Science*, 176, 2020, 108917. <http://dx.doi.org/10.1016/j.corsci.2020.108917>.
- [26] J.J. Kai, G.P. Yu, C.H. Tsai, M.N. Liu, S.C. Yao: *Metallurgical transactions A*, 20, 1989, 2057-2067. <https://doi.org/10.1007/BF02650292>.
- [27] L. Li, X.Y. Liu, X. Wang, M. Wu: *In Journal of Physics: Conference Series*, 1948(1), 2021, 012127. <https://iopscience.iop.org/article/10.1088/1742-6596/1948/1/012127>.
- [28] Q. Zhang, J. Zhang, Y. Zhuang, J. Lu, J. Yao: *Materials*, 13(9), 2020, 2128. <https://doi.org/10.3390/ma13092128>.

- [29] G.D.S. Vacchi, R. Silva, C.L. Kugelmeier, C.B. Martins Júnior, I. Dainezi, J.H. Alano, A.D.A. Mendes Filho, W.R. Ramos Osorio, C.A. Della Rovere: *Metals*, 11(8), 2021, 1286. <https://doi.org/10.3390/met11081286>.
- [30] L. Li, L. Li, G. Zhang, H. Xue, M. Cui, W. Wang, D. Liu: *Metals*, 13(6), 2023, 1069. <https://doi.org/10.3390/met13061069>.
- [31] Y. Nuñez de la Rosa, O. Palma Calabokis, V. Ballesteros-Ballesteros, C.L. Tafur, P.C. Borges: *Metals*, 13(7), 2023, 1172. <https://doi.org/10.3390/met13071172>.
- [32] S. Dewangan, S.S.S. Sunder, Y. Bhadoriya, S. Mohite, A.P. Reddy: *Journal of The Institution of Engineers (India): Series D*, 2023, 1-12. <https://doi.org/10.1007/s40033-023-00578-4>.
- [33] P.J. Ennis, A. Czyska-Filemonowicz: *Sadhana*, 28, 2003, 709-730. <https://doi.org/10.1007/BF02706455>.
- [34] W.G. Seo, J.Y. Suh, J.H. Shim, H. Lee, K. Yoo, S.H. Choi: *Materials Characterization*, 160, 2020, 110083. <https://doi.org/10.1016/j.matchar.2019.110083>.
- [35] J.B. Wen, C.Y. Zhou, X. Li, X.M. Pan, L. Chang, G.D. Zhang, F. Xue, Y.F. Zhao: *International Journal of Fatigue*, 129, 2019, 105226. <https://doi.org/10.1016/j.ijfatigue.2019.105226>.
- [36] A. Kumar, C. Pandey: *Metallurgical and Materials Transactions A*, 53(9), 2022, 3245-3273. <https://doi.org/10.1007/s11661-022-06723-0>.
- [37] V. Bhanu, C. Pandey, A. Gupta: *CIRP Journal of Manufacturing Science and Technology*, 38, 2022, 560-580. <https://doi.org/10.1016/j.cirpj.2022.06.009>.
- [38] A. Modi, N. Sharma, O. Sharma, S. Dewangan, R. Varshney: *Journal of The Institution of Engineers (India): Series D*, 2024, 1-11. <https://doi.org/10.1007/s40033-024-00668-x>.
- [39] H. Guan, W. Jiang, J. Lu, Y. Zhang, Z. Zhang: *Materials Today Communications*, 36, 2023, 106582. <https://doi.org/10.1016/j.mtcomm.2023.106582>.
- [40] Metals and Alloys: (Date of access: 22-October-2024) <https://www.phase-trans.msm.cam.ac.uk/abstracts/annealing.twin.html#note>
- [41] Carpenter Technology: (Date of access: 22-October-2024). <https://www.carpentertechnology.com/blog/nickel-base-superalloy-718-microstructure-characterization>
- [42] A. Agarwal, G. Maheshwari, Shajar, S. Dewangan: *Canadian Metallurgical Quarterly*, 2024, 1-12. <https://doi.org/10.1080/00084433.2024.2429182>.
- [43] Q. Yan, Y. Qiu, M. Yang, Q. Lu, H. Lin, M. Yang, K. Li, Y. Du: *Materials*, 16(16), 2023, 5609. <https://doi.org/10.3390/ma16165609>.
- [44] F. Ceritbinmez, A. Günen, U. Gürol, G. Çam: *Journal of Manufacturing Processes*, 89, 2023, 150-169. <https://doi.org/10.1016/j.jmapro.2023.01.072>.
- [45] L. Li, L. Li, G. Zhang, H. Xue, M. Cui, W. Wang, D. Liu: *Metals*, 13(6), 2023, 1069. <https://doi.org/10.3390/met13061069>.
- [46] J.W. Koger: *Chromium Depletion and Void Formation in Fe–Ni–Cr Alloys During Molten Salt Corrosion and Related Processes*. In: Fontana, M.G., Staehle, R.W. (eds) *Advances in Corrosion Science and Technology*. Springer, Boston, MA, 1974. https://doi.org/10.1007/978-1-4615-9059-0_4.
- [47] N. Martin, A. Hor, E. Copin, P. Lours, L. Ratsifandrihana: *Fatigue and Fracture of Engineering Materials and Structures*, 45 (4), 2022, 1258-1275. <https://imt-mines-albi.hal.science/hal-03523422v1>.
- [48] J. Li, Y. Wo, Z. Wang, W. Ren, W. Zhang, J. Zhang, Y. Zhou: *Materials*, 17(11), 2024, 2754. <https://doi.org/10.3390/ma17112754>.
- [49] X Liu, J Fan, P Zhang, K Cao, Z Wang, F Chen, D Liu, B Tang, H Kou, J Li: *Journal of Alloys and Compounds*, 930, 2023, 167522. <https://doi.org/10.1016/j.jallcom.2022.167522>.